https://doi.org/10.15407/polymerj.46.01.015
UDC 544.777:544.431.5:661.873

NATALIYA PERMYAKOVA[1*], TATYANA ZHELTONOZHSKAYA[1], DMYTRO KLYMCHUK[2], VALERIY KLEPKO[1], LIUDMYLA GRISHCHENKO[3], ARINA FOMENKO[4], LIUDMYLA VRETIK[4]
[1]Institute of Macromolecular Chemistry of the NAS of Ukraine, 48 Kharkivske highway, 02155 Kyiv, Ukraine,
[2]M.G. Kholodny Institute of Botany of the NAS of Ukraine, 2 Tereshchenkivska str., 01601 Kyiv, Ukraine,
[3]Taras Shevchenko National University of Kyiv, Faculty of Radiophysics, 4g Glushkova av., 03127 Kyiv, Ukraine,
[4]Taras Shevchenko National University of Kyiv, Faculty of Chemistry, Department of Macromolecular Chemistry, 60 Volodymyrska str., 01033 Kyiv, Ukraine,
*e-mail: permyakova@ukr.net

SYNTHESIS OF COBALT NANOPARTICLES IN AQUEOUS SOLUTIONS ASSISTED BY POLYMER/INORGANIC HYBRID

Hydrophilic polymer/inorganic hybrids (PIH) containing silica nanoparticles and polyacrylamide chains proved to be effective matrices for the in situ synthesis of cobalt nanoparticles. PIH sample was synthesized by free-radical polymerization of acrylamide from the unmodified surface of SiO_2 nanoparticles and characterized by elemental analysis, dynamic thermogravimetric analysis, static light scattering, potentiometric titration, viscometry and transmission electron microscopy (TEM). The processes of borohydride reduction of cobalt ions from the $Co(NO_3)_2 \cdot 6H_2O$ solution to nanoparticles in water medium and aqueous solutions of PIH were studied as a function of the concentrations of metal salt and hybrid concentrations using UV-Vis spectroscopy and TEM. A special approach to characterize the kinetics and efficiency of CoNPs formation in water medium and hybrid solutions using UV-Vis spectroscopy was implemented. The kinetic parameters of the CoNPs formation process as well as the yield, size, and morphology of nanoparticles in hybrid solutions and water medium at various concentrations of metal salt and hybrid were determined. The growth of both concentrations of reagents had a positive effect on the rate of formation of metal nanoparticles and their yield, but in all cases, the reduction process developed much slower in hybrid solutions compared to pure water. The morphology of the CoNPs/PIH nanocomposites was mainly represented by separate swollen hybrid particles containing metal nanoparticles with dav~3 nm.

Keywords: *polymer/inorganic hybrid, matrix, in situ synthesis, borohydride reduction, cobalt nanoparticles.*

УДК 541.64:678.07:678.65

Наталія Пермякова[1], Тетяна Желтоножська[1], Дмитро Климчук[2], Валерій Клепко[1], Людмила Гріщенко[3], Аріна Фоменко[4], Людмила Вретик[4]
[1]Інститут хімії високомолекулярних сполук НАН України, 48, Харківське шосе, Київ, 02155, Україна,
[2]Інститут ботаніки імені М.Г. Холодного НАН України, вул. Терещенківська, 2, 01601, Київ,Україна,
[3]Київський національний університет імені Тараса Шевченка, Факультет радіофізики, пр. Глушкова, 4г, 03127, Київ, Україна,

Цитування: Permyakova Nataliya, Zheltonozhskaya Tatyana, Klymchuk Dmytro, Klepko Valeriy, Grishchenko Liudmila, Fomenko Arina, Vretik Liudmila. Synthesis of cobalt nanoparticles in aqueous solutions assisted by polymer/inorganic hybrid. Polimernyi Zhurnal. 2024. **46**, no. 1: 015—029. https://doi.org/10.15407/polymerj.46.01.015

[4]Київський національний університет імені Тараса Шевченка, Хімічний факультет, Кафедра хімії високомолекулярних сполук, вул. Володимирська 60, 01033, Київ, Україна,
*e-mail: permyakova@ukr.net

СИНТЕЗ НАНОЧАСТИНОК КОБАЛЬТУ В ВОДНИХ РОЗЧИНАХ ЗА ДОПОМОГОЮ ПОЛІМЕР-НЕОРАНІЧНИХ ГІБРИДІВ

Гідрофільні полімер/неорганічні гібриди, які містять наночастинки кремнезему та поліакриламідні ланцюги (SiO_2/ПАА), виявилися ефективними матрицями для *in situ* синтезу наночастинок кобальту (CoНЧ). Зразок гібриду було синтезовано шляхом радикальної прищепленої полімеризації акриламіду від поверхні SiO_2 та охарактеризовано методами елементного аналізу, ДТГА, пружного світлорозсіювання, потенціометричного титрування, віскозиметрії. Процеси борогідридного відновлення іонів кобальту до наночастинок у водному середовищі та у водних розчинах гібриду вивчали за допомогою UV-Vis-спектроскопії та ТЕМ залежно від концентрацій солі металу та гібриду. Методом UV-Vis спектроскопії та розробленого оригінального підходу охарактеризовано кінетику й ефективність утворення CoНЧ у розчині гібриду та у водному середовищі. Встановлено кінетичні параметри процесу формування CoНЧ, а також визначено їх вихід, розмір і морфологію у гібридних розчинах та у водному середовищі за різних концентрацій солі кобальту та гібриду. Зростання обох концентрацій реагентів позитивно впливало на швидкість накопичення та вихід металевих наночастинок, але у всіх розглянутих випадках процес відновлення іонів кобальту розвивався значно повільніше в гібридних розчинах порівняно з водним середовищем. Встановлена морфологічна структура нанокомпозиту CoНЧ/гібрид, яка складалася переважно з окремих набухлих частинок гібриду, що містили металеві наночастинки середнім діаметром ~ 3 нм.

Ключові слова: полімер/неорганічний гібрид, матриця, *in situ* синтез, борогідридне відновлення, наночастинки кобальту.

Introduction

Nanostructured materials exhibit novel properties which notably differ from those of the corresponding bulk solid, due to the small size effect [1]. Cobalt nanoparticles (CoNPs) have attracted considerable attention due to their excellent magnetic properties as ferromagnetic materials. Cobalt nanomaterials are used in various fields, including catalysis, electronics, coatings, gas sensing, electrochemical devices, solar energy conversion, biomedicine including gene delivery and targeted drug carrier [2–4]. Different preparation methods have been employed for the synthesis of CoNPs, such as microemulsion, solvothermal method, thermal decomposition of cobalt precursors, spray pyrolysis, sol-gel process, plasma reduction, chemical reduction in polyol solutions [5-9], etc. These well-developed CoNPs preparation methods place high demands on the equipment due to the high temperatures, pressures or the use of organic solvents. In addition, it is difficult to control the size, size distribution, shape and stability of the metallic dispersion in these methods. The development of efficient and low-cost methods for the preparation of cobalt and cobalt oxide nanoparticles is of great interest for novel technological applications.

Chemical methods for the synthesis of CoNPs are the most widely used and at the same time, the most efficient. These methods are described as simple, convenient, inexpensive (for large-scale production), and quick to carry out while not requiring the use of complex apparatus. They are based on the use of a reducing agent, such as hydrogen, alcohol, hydrazine, borohydride, which is mixed with the metal salts in the presence of capping agents (ligands, polymers, dendrimers, surfactants, cyclodextrins, etc.) [9]. It should be noted that polymers play an important role in the preparation of CoNPs, because they control and regulate the growth of nanoparticles and prevent their aggregation. Moreover, polymers have already been widely used as steric stabilizers and as a means of controlling nanoparticles growth and spatial arrangement in films [9]. Various biocompatible hydrophilic polymers, such as dextran, proteins, polyvinyl alcohol (PVA) [10], polyvinylpyrrolidone (PVP) [11], have been previously reported for CoNP encapsulation. Cobalt and cobalt oxide nanoparticles were also obtained in hyperbranched polyester polyol matrix [12]. In addition, CoNPs for catalytic applications have been prepared in

crosslinked organic polymer microgels [13], in particular, poly(methacrylic acid) or its copolymer with poly(N-isopropylacrylamide microgels [14, 15]. In contrast to the cited works, we propose to use a polymer/inorganic hybrid (PIH) with an inorganic silica "core" and a grafted polyacrylamide "crown" for the *in situ* synthesis of CoNPs, in which the known binding properties of both components are combined and enhanced.

It is known that sodium borohydride is one of the most powerful reducing agents, which has been extensively used for the preparation and stabilization of metal nanoparticles [16], including CoNPs. Thiols, carboxylic acids, amine-based capping agents or hydrophilic polymers with -COOH, -OH and -NH_2 functional groups, which have a high ability to bind metal ions, are widely used in the stabilization of CoNPs. The borohydride reduction of Co-salt supported on natural hydrophilic polymers such as cellulose and chitosan was described in [17]. In this investigation, hydrophilic chitosan was used to improve the metal deposition on the polymer. Starch hydrogel-loaded CoNPs were prepared by *in situ* reduction of Co-salt on a starch hydrogel network [18]. In this study, CoNPs with a spherical shape and size of 30 nm were obtained. The prepared nanocomposite was applied as a heterogeneous catalyst in the reaction of hydrogen production from the hydrolysis of $NaBH_4$. The preparation of PVP-stabilized CoNPs with controllable sizes by a modified polyol method using sodium borohydride as a reducing agent has been described [9]. Borohydride reduction of Co-salt to CoNPs was also carried out in $[Co(AOT)_2]$ reverse micelles [19]. The micelles and a small volume of reducing agent play the role of nanoreactors for the nucleation and growth of CoNPs. The authors demonstrated that the amount of reducing agent is one of the key parameters in controlling the size distribution of metal nanocrystals.

Polymer/inorganic hybrids based on silica nanoparticles and grafted polyacrylamide chains contain active chemical groups that can bind to metal ions. Such chemical groups are nonionic amide groups on the grafted PAAm chains as well as ionic silanol groups on the surface of SiO_2 "cores". On the other hand, cobalt ions have a very high thermodynamic affinity for water in aqueous solutions [20]. Therefore, in an aqueous medium at a room temperature, each metal ion is surrounded by 6 water molecules, $[Co(H_20)_6]^{2+}$ [20]. As a result, hydrated metal ions interact with the active groups of low molecular weight and polymeric organic compounds, including the amide groups of PIH, through the formation of hydrogen bonds via water molecules [21]. A different situation is observed at a higher temperature (~80 °C), when cobalt ions "lose" water molecules and interact with amide groups through ion coordination bonds [22].

The formation of coordination complexes of transition metals with PAAm amide groups is well known in the literature [22-27]. As a ligand, acrylamide (AAm) can form monodentate O- or N-bonded complexes with metal ions, as well as bidentate chelate rings or bridging complexes [23, 24]. The most basic site in AAm based ligands is oxygen, where protonation or metallation occurs in neutral conditions. In general, changes in the acidity and oxidation states of the metal center, substituent group, temperature, moisture and solvent system influence the stability and coordination mode in metal-AAm ligand complexes. Metal ions such as Cr^{3+}, Co^{3+}, Ru^{3+}, Rh^{3+} and Cu^{2+}, $Co^{2+,}$ Fe^{2+} favor O-bonded amide complexation [24]. It should be noted that hydrogen-bonded complexes of hydrated cobalt ions with amide groups of PAAm are pink in color at room temperature. At the same time, the ion coordination binding of cobalt ions with the amide groups of PAAm at higher temperature (T=85 °C) leads to the formation of insoluble blue complexes [25].

The present work reports a simple and effective method for the preparation of small and stable to aggregation and sedimentation CoNPs in an aqueous medium using polymer/inorganic hybrid SiO_2/PAAm based on silica nanoparticles and grafted polyacrylamide chains. Previously, such hybrids were shown to be effective nanoreactors for the *in situ* synthesis of silver nanoparticles (AgNPs) in an aqueous medium [28, 29]. It was concluded that the strong retention of metal ions and the resulting nanoparticles in hybrid particles is due to the presence not only of PAAm "corona" with active primary amide groups but also of silica "core" with a weakly negatively charged surface. The present work is mainly devoted to the kinetic peculiarities and efficiency of CoNP formation in PIH solutions in comparison with pure water at various concentrations of Co precursor and hybrid matrix using the previously developed method [30]. However, a comparison of the morphology and size of the resulting CoNPs was also performed.

Experimental part

Synthesis and characterization of polymer/inorganic hybrid

The PIH sample was synthesized by a free-radical grafting polymerization of acrylamide (AAm) "from" the surface of silica hydrosol, as in the study [28–30]. For this purpose, we used Aerosil A-175 from "Orisil" (Ukraine) with a specific surface area of $1.82 \cdot 10^5$ $m^2 \cdot kg^{-1}$, ammonium cerium(IV) nitrate from "Aldrich" (USA) and AAm from "Merck" (Germany), which was recrystallized from chloroform. To prepare a silica hydrosol, the Aerosil suspension was stirred in deionized water with C=100 $kg \cdot m^{-3}$ during 24 hours and then centrifuged twice at 6000 rpm. The concentration of silica sol in the supernatant was measured by the gravimetric method, and the average nanoparticle size (R_{SiO2}) was determined by static light scattering [30]. The weight ratios: $[Ce^{IV}]/[SiO_2]$=0.4 and $[Ce^{IV}]/[AAm]=7.72 \cdot 10^{-3}$, which determined the quantity and length of the grafted chains, and the concentration of C_{SiO_2}=2.7 $kg \cdot m^{-3}$ were used. The reagents were mixed in an inert atmosphere at 293 K for 24 hours. The gel-like product was diluted, precipitated with acetone, redissolved in water and freeze-dried.

A detailed structure of the hybrid was determined by elemental analysis, dynamic thermogravimetric analysis (DTGA) and viscometry. Elemental analysis data for C and N were used to determine the weight fraction of PAAm in PIH. The weight part of water was determined according to DTGA as the weight loss of a hybrid sample prior to the onset of degradation. Based on these results, the weight fraction of SiO_2 was calculated. To determine the number and molecular weight of the grafted PAAm chains, the PIH solution was kept at pH=11.5 and room temperature for one week. It is known that under such conditions a complete degradation (dissolution) of silica nanoparticles occurs [31] and only a slight hydrolysis of PAAm acrylamide units can be observed [32]. The reaction mixture was then reprecipitated with acetone and dissolved in water. The degradation products were completely separated from the polymer chains by dialysis of the solution against deionized water, and the average molecular weight of the grafts was determined using the well-known method of viscometry.

The viscosity was measured in diluted aqueous solutions of PAAm (C_{PAAm}=0.1–1.0 $kg \cdot m^{-3}$) at T=303±0.1 K in the presence of $NaNO_3$ (C_{NaNO_3}=1 M) as a low molecular weight electrolyte to suppress possible polyelectrolyte effect caused by partial hydrolyses of acrylamide units. We used the Ostwald-type viscometer with the water-salt solution flow time τ_0=93.5 s. The resulting linear dependence of the reduced viscosity of the polymer solution on its concentration was used to determine the intrinsic viscosity ([η]) and to calculate the viscosity-average molecular weight of PAAm using the equation (1):

$$[\eta] = 3.73 \cdot 10^{-2} \cdot M^{0.66}_{vPAAm}, \quad (1)$$

where [η] was expressed in $cm^3 \cdot g^{-1}$.

The obtained characteristics made it possible to calculate the number of PAAm grafts (N) per one SiO_2 nanoparticle according to the formula (2):

$$N = \frac{4\pi \cdot R^3_{SiO2} \cdot \rho \cdot w_{PAAm} \cdot N_A}{3 \cdot w_{SiO2} \cdot M_{vPAAm}}, \quad (2)$$

where ρ=2.1 $g \cdot cm^{-3}$ is the density of silica, the product $4/3\pi \cdot R_{SiO_2}{}^3 \cdot \rho$ is the weight of one silica nanoparticle, N_A is the Avogadro number. The results of calculations are shown in table.

Methodology of *in situ* synthesis of cobalt nanoparticles

In order to obtain CoNPs, we performed *in situ* reduction of cobalt(II) nitrate hexahydrate, $Co(NO_3)_2 \cdot 6H_2O$ (Merk, Germany), with $NaBH_4$ (Aldrich, Germany) as reducing agent in hybrid aqueous solutions at T=20 °C. All the chemical re-

Table. **Main characteristics of the hybrid sample**

Sample	w_{SiO_2} [a], w %	$R_{av\ SiO_2}$ [b], nm	w_{PAAm} [c], w %	$M_{v\ PAAm}$ [d], kDa	w_{H_2O} [e], w %	N [f]
PIH	9.5	7.7	85.5	822	11	72

[a] The weight fraction of SiO_2 in the hybrid: $w_{SiO_2}=1-w_{PAAm}-w_{H_2O}$; [b] Average radius of silica nanoparticles foundby static light scattering; [c] The weight fraction of PAAm in the sample, calculated according to elemental analysis; [d] Viscosity-average molecular weight of the grafted PAAm chains; [e] Total water content in the sample, determined by DTGA; [f] The average quantity of PAAm grafts per particle SiO_2.

agents used in the experiment were of analytical grade and were used without further purification. The aqueous solutions of the reagents were prepared using deionized water at pH=6.5. The formation of CoNPs in aqueous PIH solutions was carried out in two stages. In the first stage, Co-salt of the required concentration was added to the PIH solution in deionized water. The Co-salt/PIH mixture was then stored in a dark box for 1 hour. In the second stage, twenty-fold molar excess of $NaBH_4$ was added to the mixture to achieve the complete conversion of metal ions to zero-valence state. In the experiments, the concentrations of the hybrid matrix (C_m) and Co-salt solutions were varied (C_m = 0.5–2.0 kg·m^{-3}; $C_{Co(NO_3)_2}$ = 0.98–3.92·10^{-2} kg·m^{-3}). It should be noted that the concentration of Co-salt in the article is expressed based on pure cobalt nitrate without water. To determine the peculiarities of the CoNP formation without polymer/inorganic matrix stabilization, we carried out the reduction of Co-salt aqueous solution by $NaBH_4$ in deionized water under similar experimental conditions.

The process of CoNP formation was monitored over time by changes in the extinction (turbidity) of each reaction mixture at λ=500 nm. At this wavelength, the Co-salt and PIH solutions had no absorption bands in the spectrum, and the main contribution to the extinction value was made by the scattering of light by the metal nanoparticles. Extinction spectra were recorded every 2 minutes for 1.5 hours in the 200-1000 nm range using a Cary 50 Scan UV-Vis spectrometer (Varian, USA). The extinction values (optical density D) at a wavelength of λ=500 nm were then used to calculate the turbidity (τ) of each reaction mixture as a function of time (t) according to the well-known formula (3):

$$\tau(t) = 2.303\frac{D(t)}{l}, \qquad (3)$$

where l=1 cm is the length of the quartz cuvette.

Determination of the morphology and size of hybrid and metal nanoparticles

The morphology and size of CoNPs obtained in water medium and PIH solutions were determined using transmission electron microscopy (TEM). The nanoparticles produced in water were studied by TEM as prepared. To study the CoNPs/PIH composites, we previously purified them from the reaction by-products by means of their reprecipitation with ethanol and subsequent redissolution with deionized water. Corresponding TEM images were obtained using a JEM-1230 instrument (JEOL, Japan) operating at an accelerating voltage of 90-100 kV. Small droplets (~1·10^{-4} cm^3) of the dispersions were placed on copper grids coated with Formvar films and carbon, and then dried in air for ~1-2 min and in a vacuum desiccator for 24 h. The average particle diameter (d_{av}) and their size distribution for PIH solutions and CoNPs/PIH composites, as well as for CoNPs obtained in water medium, were calculated from the TEM images using ImageJ computer program

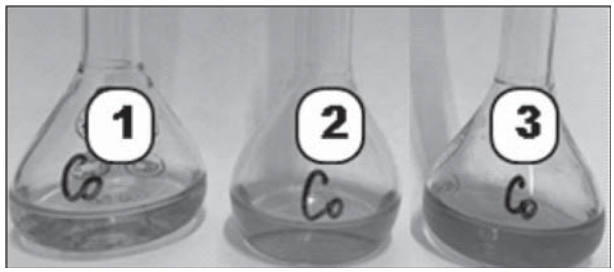

Fig. 1. Co-salt aqueous solutions with increasing $Co(NO_3)_2$ concentration in 10 minutes after the addition of $NaBH_4$. $C_{Co(NO_3)_2}$=0.98·10^{-2}– *1*; 1.96·10^{-2} – *2* and 3.92·10^{-2} kg·m^{-3} – *3*; T=20 °C

Results and discussion

Process of cobalt nanoparticle formation in water medium

Borohydride reduction of metal ions has been used extensively to form metal particles, yielding either zero valence metals or particles of metal borides [33, 34]. Sodium borohydride is a mild but effective reducing agent with low equivalent weight and high reduction potential (E°= -1.23 V). It has been successfully used for *in situ* synthesis of noble metal nanoparticles [28, 29, 35]. In recent years, this method has gained on additional importance due to the increased interest in nanoscale magnetic particles. However, unlike gold and silver, cobalt nanoparticles are sensitive to air, moisture and reaction conditions. The redox potential of the Co^{2+}/Co^0 pair is -0.28 V [34]. The overall reaction scheme of the reduction process in aqueous medium was proposed as follows:

$$Co^{2+} + 2BH_4^- + 6H_2O \rightarrow Co° + 7H_2 + 2B(OH)_3$$

Complete reduction of cobalt ions by this technique requires a significant excess of borohydride [33].The interaction of these ions with sodium

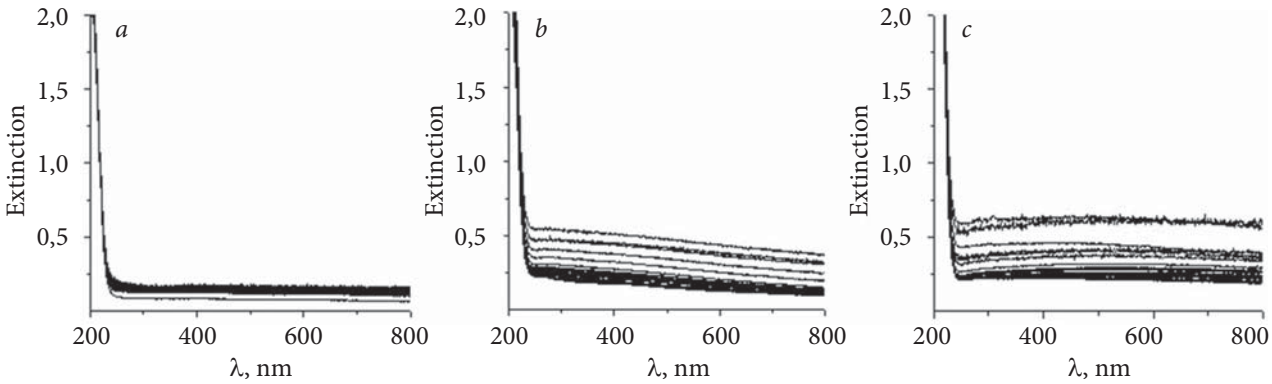

Fig. 2. The time evolution over 90 min of the extinction spectra of the Co-salt aqueous solutions after the addition of $NaBH_4$. The spectra are shown with an interval in 4 min. $C_{Co(NO_3)_2}$= 0.98·10^{-2} (*a*), 1.96·10^{-2} (*b*) and 3.92·10^{-2} kg·m^{-3} (*c*); *T*=20 °C

borohydride in water in an inert atmosphere results in the formation of cobalt boride [33]:

$$2Co^{2+}+2BH_4^-+2H_2O \rightarrow Co_2B+HBO_2+2H^++4.5H_2$$

In air, however, a Co_2B is converted to CoNPs due to the interaction with oxygen according to the following reactions [33]:

$$4Co_2B + 3O_2 = 8Co° + 2B_2O_3 ;$$
$$B_2O_3 + 3H_2O = 2B(OH)_3$$

The reaction mixtures Co-salt/$NaBH_4$ with increasing concentration of reagents are shown in Figure 1. In this experiment, a twenty-fold excess of $NaBH_4$ was added to aqueous $Co(NO_3)_2 \cdot 6H_2O$ solutions of various concentrations.

When the reducing agent was added, a gray-black color appeared in all colorless mixtures of Co-salt/$NaBH_4$ within a few minutes, thus reflecting the occurrence of CoNPs. It can be seen that the yield of nanoparticles increased with the increase of salt concentration (and reducing agent).

The extinction spectra of the initial aqueous Co-salt solutions with various concentrations after the addition of $NaBH_4$ are shown in Figure 2. The formation of CoNPs dispersions occurred at a high rate that was especially evident at $C_{Co(NO_3)_2}$=1.96·10^{-2} and 3.92·10^{-2} kg·m^{-3} (Figure 2 b, c).

The formation and yield of noble metal nanoparticles, such as silver and gold, in various media can be easily controlled using UV-Vis spectroscopy due to the appearance of intense surface plasmon resonance bands (SPRB) with λ_{max}~400 nm and ~520 nm, respectively [36,37]. Therefore, we have used this method in previous studies to characterize the kinetics of silver nanoparticles formation and their yield during borohydride reduction of Ag^+ ions in aqueous solutions of double-hydrophilic block copolymers and polymer/inorganic hybrids [28, 29, 35]. To this end, the changes in the position and integrated intensity of the SPRB of silver nanoparticles in the UV-Vis spectra of the corresponding reaction mixtures were monitored over time. In contrast, the SPRB of CoNPs in our dispersions is poorly expressed (Fig. 2), which can be attributed to the less free state of surface electrons. Nevertheless, this band was found for CoNPs at 350 nm (SPRB1) and 430 nm (SPRB2) in organic media [38], but its position and intensity strongly depended on the size and shape of the nanoparticles, and on the dielectric properties of

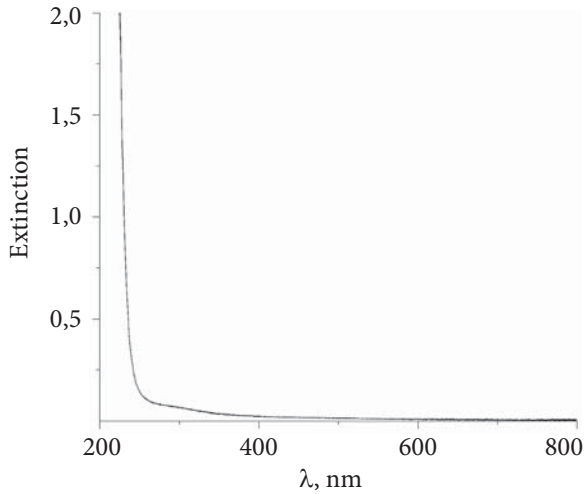

Fig. 3. Time evolution of the extinction spectrum of the Co-salt/PIH mixture with the maximum concentrations of the components over 90 min. C_m=2 kg·m^{-3}, $C_{Co(NO_3)_2}$=3.92·10^{-2} kg·m^{-3}, *T*=22 °C

the environment. In the present study, we also did not observe the appearance of SPRB in the UV-Vis spectra during the preparation of CoNPs in water medium and aqueous PIH solutions (in the selected range of reagent concentrations). Therefore, we proposed another way to characterize the kinetics and efficiency of the reduction process [30, 39]. To solve this problem, such a parameter as turbidity of the reaction mixture at λ=500 nm was chosen. At this wavelength, the solutions of Co-salt and its mixtures with hybrid did not show any absorption bands in the spectra (Fig. 3).

It is known that the turbidity of colloidal dispersions, which characterizes the scattering of light by them, can be expressed for small (<λ/20 of the incident light) spherical particles by the equation (4) [40]:

$$\tau = -\frac{1}{l}\ln\left(\frac{I_t}{I_0}\right) = 2.303\frac{D}{l} = \left(\frac{N}{V}\right)\frac{128\cdot\pi^5\cdot a^6}{3\cdot\lambda^4}\left(\frac{n^2-1}{n^2+2}\right), \quad (4)$$

where: I_0 and I_t are the intensities of the incident and transmitted light, N/V is the number of particles per unit volume of the dispersion, a is the radius of the spherical particles, $n=n_1/n_2$ is the relative refractive index or the ratio of the refractive indices of particles and the medium.

Thus, the turbidity of the dispersion is determined by the size and number of scattering particles; therefore, its change can characterize the rate and effectiveness of the reduction process. Given the formation of very small spherical CoNPs in all our reduction processes, this parameter was used to control the appearance of nanoparticles in the reaction mixtures. Thus, the control of CoNP formation in water medium and also in PIH solutions after the addition of reducing agent was performed by monitoring the time changes in the extinction spectra of the reaction mixtures (Fig. 2) followed by the determination of the corresponding time dependences of the turbidity (τ) of the mixtures at λ=500 nm.

The resulting kinetic curves of the CoNP formation in water medium, calculated from the corresponding extinction spectra (Fig. 2), are shown in Fig. 4. It is seen that the yield of CoNPs in water without hybrid matrix increased with increasing concentration of cobalt ions (and $NaBH_4$) in the reaction mixture. The formation of CoNPs in solutions with high concentrations of Co-salt ($1.96\cdot10^{-2} \div 3.92\cdot10^{-2}$ kg·m^{-3}) was accompanied by the processes of nanoparticle aggregation and possibly partial sedimentation (Fig. 4*b*, *c*).

The appearance of small, but well-formed spherical CoNPs, was confirmed by TEM (Fig. 5 *a*, *b*). Nanoparticles obtained at lower concentration of Co-salt solutions had smaller average particle diameter d_{av}=2.0±0.8 nm (Fig. 5 *c*). In contrast, CoNPs formed at higher concentration of Co-salt (and reducing agent) were slightly larger (Fig. 5 *d*) with d_{av}=2.7±1.5 nm and had a wider size distribution.

Formation and stabilization of cobalt nanoparticles in aqueous hybrid solutions

The hydrophilic PIH form compact micelle-like structures in the aqueous medium, in which the polymer "corona" is pressed to the inorganic "core" due to an additional system of hydrogen bonds between the PAAm chains and the silica surface [28–30]. The aqueous PIH solutions have a pH~6. These compact hybrid particles exist in both an individual and in an aggregated state in aqueous solutions. The morphology and size distribution of the synthesized hybrid sample are shown in Fig. 6.

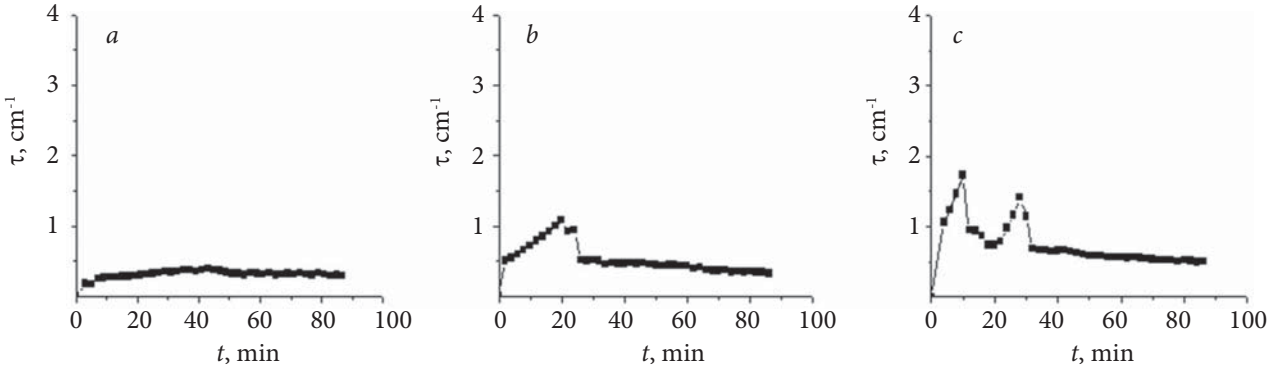

Fig. 4. Turbidity changes over 90 min in the Co-salt solutions after $NaBH_4$ addition. $C_{Co(NO_3)_2}$ = $0.98\cdot10^{-2}$ (*a*), $1.96\cdot10^{-2}$ (*b*) and $3.92\cdot10^{-2}$ kg·m^{-3} (*c*); *T*=20 °C

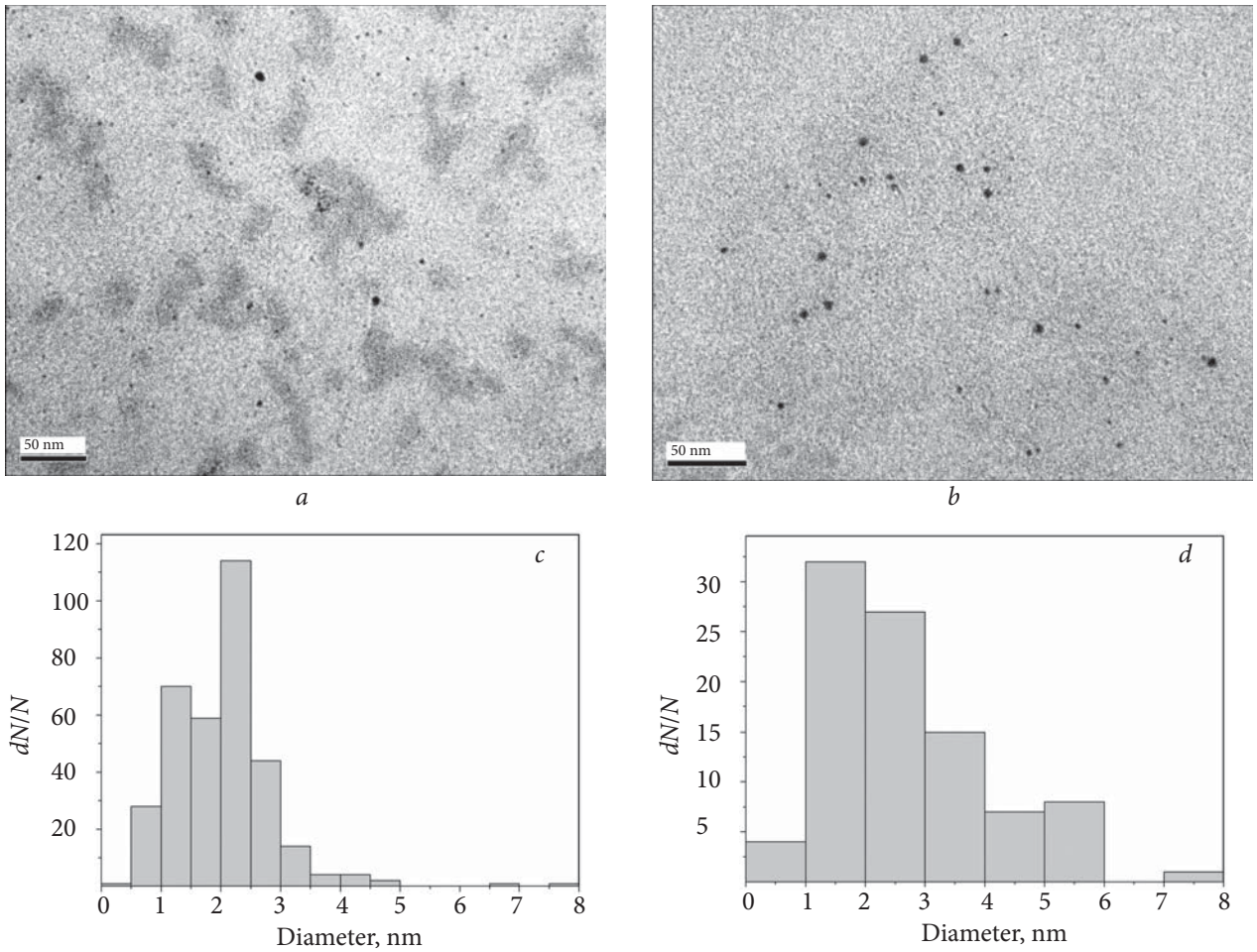

Fig. 5. TEM images of CoNPs obtained in water medium at different initial concentration of Co-salt solution (*a*, *b*) and particle size distribution (*c*, *d*). $C_{Co(NO_3)_2}$ = 1.96·10^{-2} (*a*, *c*) and 3.92·10^{-2} kg·m^{-3} (*b*, *d*); *T*=20 °C

The small individual hybrid particles had an almost spherical shape and the average diameter d_{av}=21.0±4.7 nm. These particles are combined into various fractal aggregates of different shapes and sizes. The reason for the aggregation of hybrid particles in an aqueous solution seems to be is the

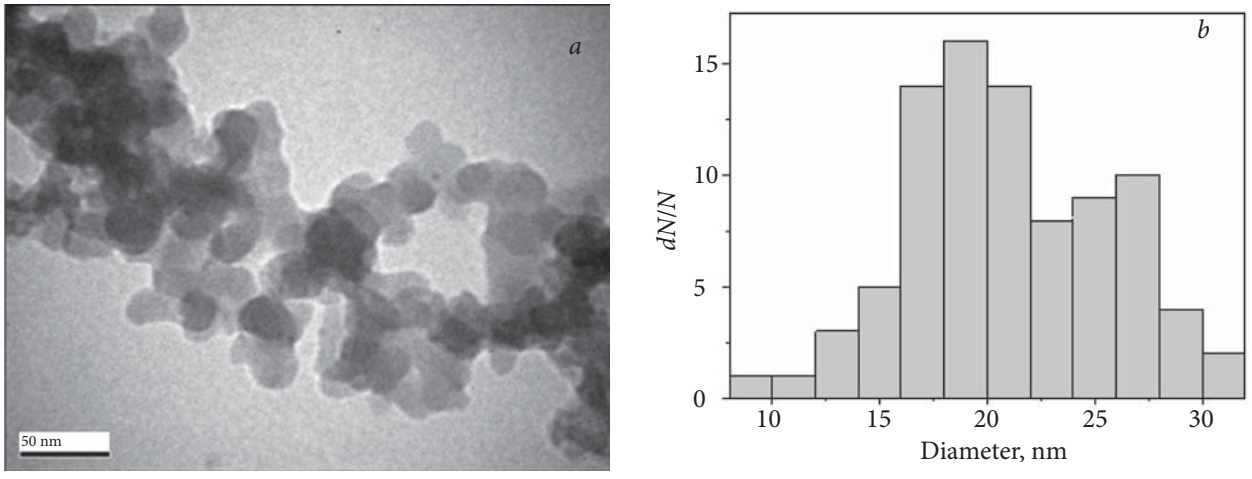

Fig. 6. TEM image of PIH matrix obtained using aqueous solution (*a*) and particle size distribution (*b*). C_m=1.0 kg·m^{-3}; *T*=20 °C

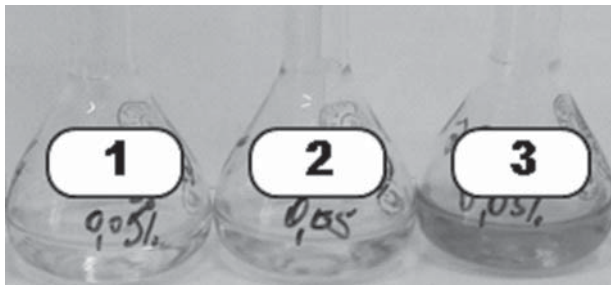

Fig. 7. Co-salt/PIH mixtures in 45 minutes after the addition of $NaBH_4$. C_m=0.5 kg·m^{-3}; $C_{Co(NO_3)_2}$=0.98·10^{-2}– *1*; 1.96·10^{-2} – *2* and 3.92·10^{-2} kg·m^{-3} – *3*; *T*=20 °C

interaction of PAAm "coronas" due to the hydrogen bonds.

The reaction of borohydride reduction of Co-salt in PIH solutions was divided into two separate stages accordint to the previously developed methodology for the *in situ* synthesis of AgNPs in hybrid solutions [28, 29]. In the 1st stage, the hydrated cobalt ions $[Co(H_2O)_6]^{2+}$ penetrated into the PIH particles and interacted with the primary amide groups of PAAm through hydrogen bonds and, possibly, with the partially negatively charged

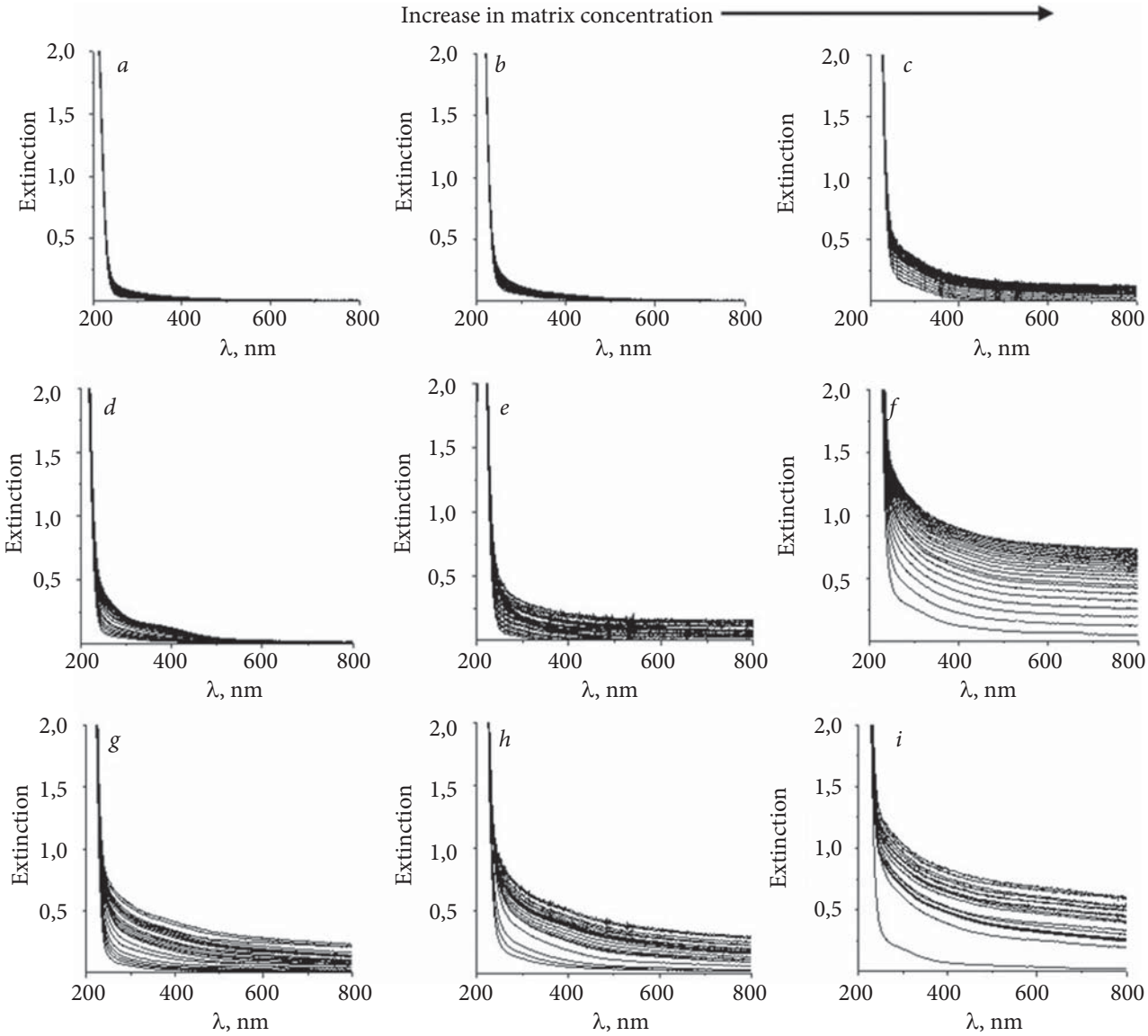

Fig. 8. Extinction spectra of the Co-salt/PIH mixtures after $NaBH_4$ addition. The spectra are shown over 90 minutes with an interval of 4 min. $C_{Co(NO_3)_2}$ = 0.98·10^{-2} (*a*, *b*, *c*), 1.96·10^{-2} (*d*, *e*, *f*) and 3.92·10^{-2} kg·m^{-3} (*g*, *h*, *i*); C_m 0.5 (*a*, *d*, *g*), 1.0 (*b*, *e*, *h*) and 2.0 kg·m^{-3} (*c*, *f*, *i*); *T*=20 °C

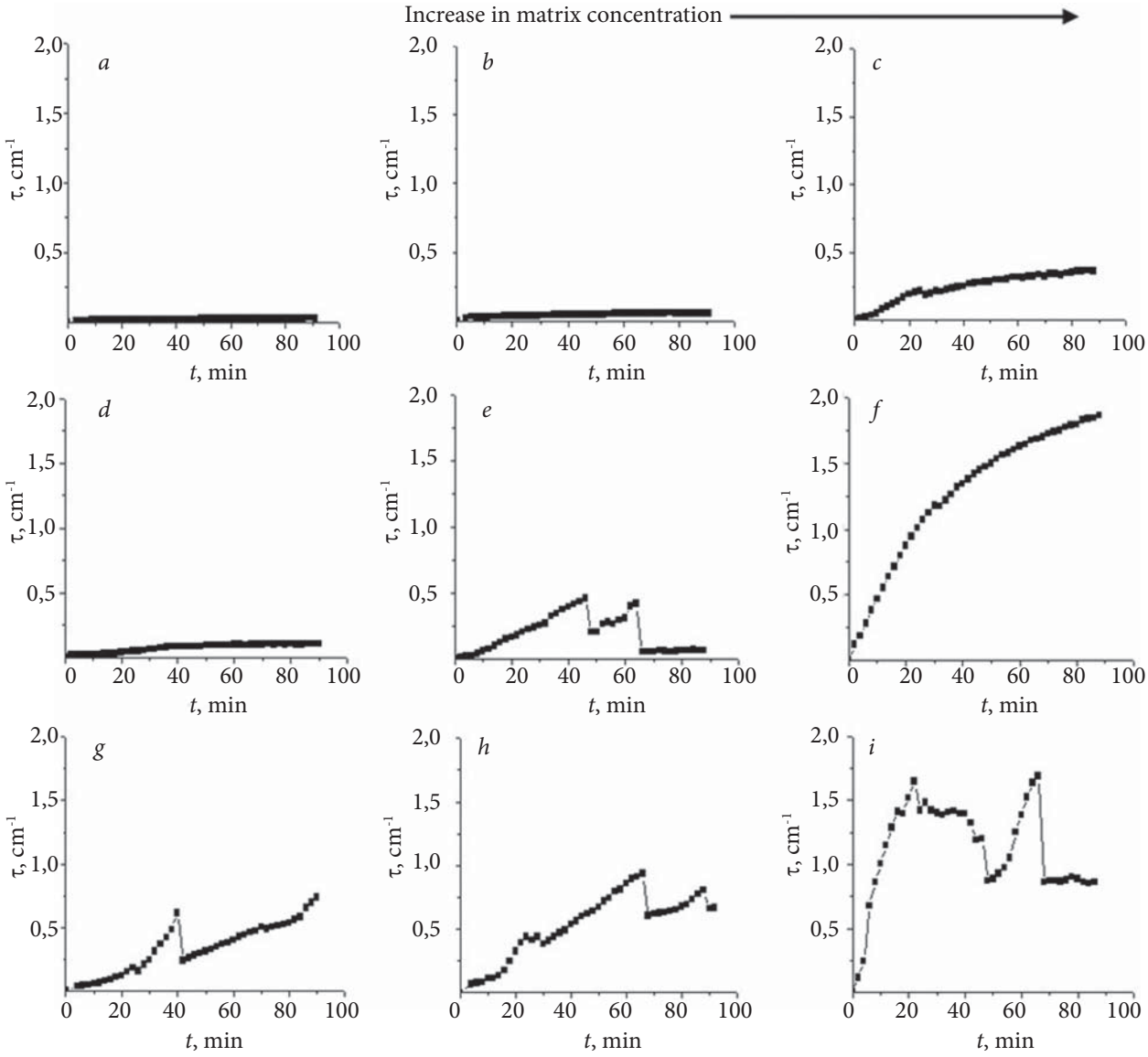

Fig. 9. Turbidity changes over 90 min in the Co-salt/PIH mixtures after reducing agent addition. $C_{Co(NO_3)_2}$ = 0.98·10^{-2} (*a*, *b*, *c*), 1.96·10^{-2} (*d*, *e*, *f*) and 3.92·10^{-2} kg·m^{-3} (*g*, *h*, *i*); C_m = 0.5 (*a*, *d*, *g*), 1.0 (*b*, *e*, *h*) and 2.0 kg·m^{-3} (*c*, *f*, *i*); *T*=20 °C

surface of SiO_2 particles through electrostatic interactions. Thus, in the 1st stage the metal ions were connected with the matrix particles. It was previously shown, that in an analogous synthesis of nanosilver, the formation of AgNPs occurred in the PAAm grafted layer [28, 29].

In the 2nd stage, when the reducing agent was added, a gray-black color appeared in all colorless Co-salt/PIH mixtures within ~10 minutes, thus reflecting the occurrence of CoNPs (Fig. 7). It can be seen that the yield of nanoparticles increased with the growth of the Co-salt (and the reducing agent) concentrations at a constant hybrid concentration.

The extinction spectra of all reaction mixtures of PIH with cobalt ions after the addition of $NaBH_4$ are shown in Figure 8. The extinction values in the spectra monotonically decreases to the long-wavelength region from an intense Co^0 absorption band nearly λ~200 nm [41].

Note, that the oxygen-containing amide and silanol groups of the hybrid also have absorption bands near 200 nm. All figures show the shift of the extinction spectra for 90 min compared to the initial spectrum, thus indicating an increase in turbidity of the systems over time due to the scattering of light by the forming CoNPs. At the same time, no distinct surface plasmon resonance band for CoNPs was observed in any of the spectra. The

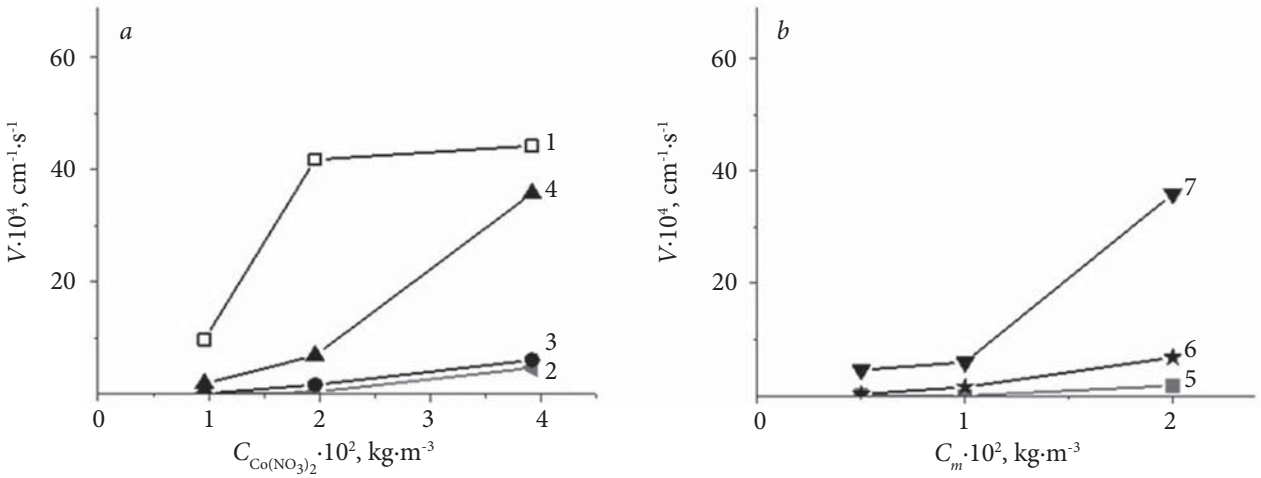

Fig. 10. The changes in the rate of accumulation of NPs at: Co-salt concentration at the constant concentration of matrix (*a*) and PIH concentration at the constant concentration of metal salt (*b*). C_m = 0 (*1*), 0.5 (*2*), 1.0 (*3*) and 2.0 (*4*) kg·m^{-3} (*a*); $C_{Co(NO_3)_2}$ = 0.98·10^{-2} (*5*), 1.96·10^{-2} (*6*), 3.92·10^{-2} (*7*) kg·m^{-3} (*b*); *T*=20 °C

increase of the matrix concentration at all studied concentrations of $Co(NO_3)_2$ had a positive effect on the yield of CoNPs, which was evidenced by the increase of the shift of the extinction spectra compared to the initial spectrum with increasing C_m (Figure 8 *c*, *f*, *i*). As noted above, the process of CoNPs formation was controlled by changes in the turbidity of the dispersions over time. The kinetic curves of the turbidity changes in time for the Co-salt/PIH/$NaBH_4$ mixture are shown in Fig. 9.

The yield of metal nanoparticles under different conditions can be characterized from Fig. 9 as the turbidity value over a certain constant time (80 minutes), τ_{80}. These data already quantitatively confirmed the previous conclusions that the yield of CoNPs in hybrid solutions at a constant hybrid

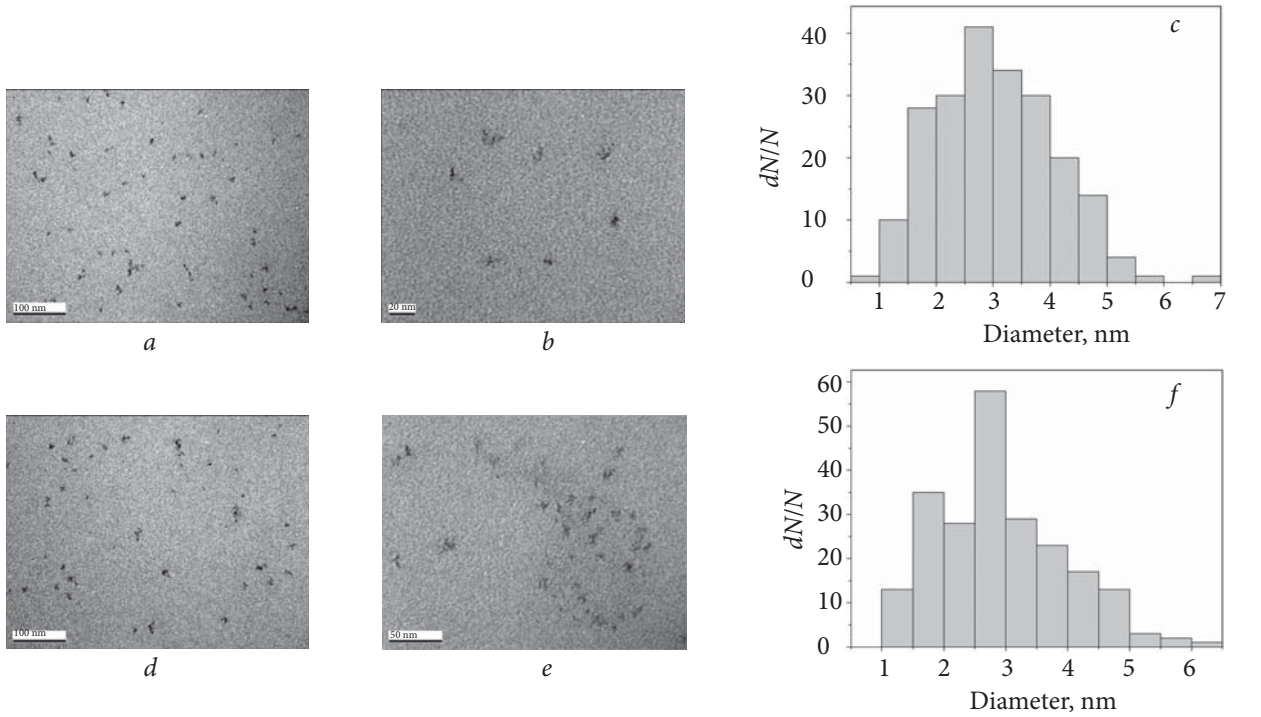

Fig. 11. TEM images of CoNPs, obtained in hybrid solutions at different magnifications and initial Co-salt concentrations (*a*, *b*, *d*, *e*), and particle size distribution (*c*, *f*). $C_{Co(NO_3)_2}$ 1.96·10^{-2} (*a*, *b*, *c*) and 3.92·10^{-2} kg·m^{-3} (*d*, *e*, *f*); C_m=2.0 kg·m^{-3}; *T*=20 °C

concentration increases with increasing of the Co-salt concentration (Fig. 9 *a*, *d*, *g*; *b*, *e*, *h*; *c*, *f*, *i*). A similar effect of growth of CoNPs yield in hybrid solutions we also observe with increasing concentration of the hybrid at a constant Co-salt concentration (Figure 9 *a*, *b*, *c*; *d*, *e*, *f*; *g*, *h*, *i*). As can be seen, the CoNP formation is a complex stochastic process involving aggregation and possible partial sedimentation of disperse particles in a measuring cell. In addition, the reduction reaction is accompanied by the release of small hydrogen bubbles. For this reason, some kinetic curves are complicated by fluctuations in the value of τ or even by its decrease after the maximum. The analysis of the experimental data in Fig. 9 allows the determination of the optimal concentrations of the hybrid matrix and Co-salt, at which the highest yield and stability of nanoparticles in solution are obtained. According to Fig. 9 (*f*)**,** the optimal concentrations for hybrid matrix and Co-salt (based on pure cobalt nitrate) were 2 kg·m^{-3} and 1.96·10^{-2} kg·m^{-3} respectively.

The rates of nanoparticle accumulation (V) of CoNPs in hybrid solutions and water medium were calculated from the curves in Fig. 4, 9 as the slopes of the initial sharp increase in the turbidity of every system over time. The process of borohydride reduction of Co-salt in pure water started almost immediately without any induction period (Fig. 4). In contrast, the process of nanoparticle formation in the hybrid solutions began after a moderate induction period in most cases (Fig. 9). Analysis of the data in Fig. 9 also shows a clear tendency for the length of the initial period of nanoparticle nucleation to decrease with increasing concentration of the hybrid matrix.

The dependencies of the rate of the CoNP accumulation on the both concentrations of reagents (on Co-salt and hybrid concentrations) are shown in Fig. 10. Obtained the results indicate an increase in CoNPs formation rate and yield with increasing concentrations of both reagents. Thus, the growth of both concentrations had a positive effect on the rate of CoNPs formation and the yield of nanoparticles, but in all cases the reduction process of Co-salt in hybrid solutions developed much slower (Fig. 10*a*, curves *2–4*) compared to the borohydride reduction of metal ions in water medium (Fig. 10*a*, curve *1*).

TEM images of the obtained CoNPs/PIH compositions, which were pre-cleaned from the reaction by-products, and their particle size distributions are shown in Fig. 11.

The TEM images of all the studied composites showed the presence of mainly isolated swollen hybrid particles and only a few diffuse particle aggregates. The isolated swollen particles of PIH contained small are clearly visible metal nanoparticles at both concentrations of Co-salt (Fig. 11 *a*, *d*, *c*, *f*). The average diameters of CoNPs obtained at $C_{Co(NO_3)_2}$=1.96·10^{-2} and 3.92·10^{-2} kg·m^{-3} were close: d_{av}=3.0±1.0 nm and d_{av}=2.9±1.0 nm, respectively. Note, that the CoNPs, obtained in hybrid solutions, had a slightly higher average size as compared to the CoNPs obtained in water medium. However, the yield of nanoparticles (the τ_{80} values), which capable of being kept in solution, is much higher in the presence of hybrid matrices due to their binding and stabilizing action. Thus, the individual particles of the hybrid matrix with CoNPs can be considered as the basic structural elements of such nanocomposites in solution.

The TEM images of all the studied compositions showed a similar picture, which we observed during the borohydride reduction of $AgNO_3$ in aqueous PIH solutions. In particular, the similar synthesis of AgNPs showed a slight swelling of the hybrid particles. Silver ions penetrated into the "corona" of PIH due to the complex formation with amide groups of PAAm and probably with a weakly negatively charged surface of SiO_2. Therefore, the process of AgNP formation with further addition of reducing agent already developed in the "corona" of hybrids and was accompanied by significant destruction of the initial fractal clusters of PIH. Obviously, a similar process developed in the case of Co-salt reduction in PIH solutions.

The resulting highly dispersed CoNPs/PIH nanocomposites, similar to AgNPs/PIH nanocomposites, were resistant to aggregation and sedimentation over time. However, unlike the latter, they showed some changes in the color of the metal nanoparticles. The initial black color of the dispersed systems gradually changed to dark brown, and they became more transparent. This indicated chemical transformations on the surface of CoNPs, as the presence of metal nanoparticles in these composites was confirmed by TEM. The reasons and directions of chemical transformations, as well as issues of chemical stabilization of the surface of CoNPs in such nanocomposites, will be considered separately in our next publications.

Conclusion

The present work demonstrates the preparation of CoNPs assisted with polymer/inorganic hybrid containing PAAm chains grafted on the surface of SiO_2 nanoparticles. The *in situ* synthesis of CoNPs in PIH solutions developed mainly in grafted PAAm chains, resulting in the formation of a water-stable nanocomposites comprised of swollen hybrid particles with small (d_{av}~3 nm) spherical CoNPs in the PAAm polymer "corona".

The formation of CoNPs was monitored over time by the changes in the extinction spectra of the $Co(NO_3)_2 \cdot 6H_2O$ in PIH aqueous solutions or water medium after $NaBH_4$ addition. The reaction kinetics was determined from the changes in the turbidity of the forming metal dispersions at the λ = 500 nm. An increase in the rate of accumulation and yield of CoNPs with increasing of both Co-salt and matrix concentrations was observed. It was found the optimal concentrations of hybrid matrix and Co-salt (2 $kg \cdot m^{-3}$ and $1.96 \cdot 10^{-2}$ $kg \cdot m^{-3}$ respectively), at which a high yield and stability of CoNPs in the final composite was achieved. In water medium, the rate of accumulation and the yield of CoNPs also increased with the increase of Co-salt concentration. In addition, at each salt concentration, this rate was significantly higher compared to the CoNPs formation in PIH solutions. However, the resistance of nanoparticles, obtained in an aqueous environment, to aggregation and sedimentation is significantly lower compared to nanoparticles synthesized in aqueous solutions of PIH. Thus, the growth process of CoNPs in PIH matrices under the influence of a reducing agent is slowed down and becomes more controlled.

REFERENCES

1. *Romero-Fierro D., Bustamante-Torres M., Bravo-Plascencia F., Magaña H., Bucio E.* Polymer-Magnetic Semiconductor Nanocomposites for Industrial Electronic Applications. Polymers, 2022, 14: 2467-2490. https://doi.org/10.3390/polym14122467.
2. *Li X., Sun L., Wang H., Xie K., Long Q., Lai X., Liao L.*Synthesis of cobalt nanowires in aqueous solution under an external magnetic field. Beilstein J. Nanotechnol. 2016, **7**: 990-994. https://doi.org/10.3762/bjnano.7.91.
3. *Vodyashkin A.A., Kezimana P., Prokonov F.Y., Vasilenko I.A., Stanishevskiy Y.M.* Current Methods for Synthesis and Potential Applications of Cobalt Nanoparticles: A Review. Crystals, 2022, **12**: 272-298. https://doi.org/10.3390/cryst12020272.
4. *Kaur A., Gangacharyulu D., Bajpai P.K.* Catalytic Hydrogen Generation from NaBH4/H2O System: Effects of Catalyst and Promoters. Brazilian Journal of Chemical Engineering, 2018, **35**,№1: 131-139. https://doi.org/10.1590/0104-6632.20180351s20150782.
5. *Angeloni L., Passeri D., Schiavi P.G., Pagnanelli F., Rossi M.* Magnetic force microscopy characterization of cobalt nanoparticles: A preliminary study. International conference of trends in material science and inventive materials: ICTMIM 2020. https://doi.org/10.1063/5.0023608.
6. *Dzidziguri E.L,Sidorova E.N, Inkar M., Yudin A.G., Kostitsyna E.V., Ozherelkov D.Yu., Slusarsky K.V., NalivaikoA.Yu., Gromov A.A.* Cobalt nanoparticles synthesis by cobalt nitrate reduction. Mater. Res. Express, 2019, **6**: 105081. https://doi.org/10.1088/2053-1591/ab3ca8.
7. *Zhang Z., Zhou T., Lu M., Poh A.W.C., Piramanayagam S.N.* Cobalt Nanomaterials: Synthesis and Characterization. In: Nanotechnologies for the Life Sciences. Edited by Challa S.S.R. Kumar WILEY-VCH Verlag GmbH & Co. KGaA, Weinheim. 2011, 4680 pp.
8. *Anwar A., Numan A., Siddiqui* R., *Khalid M., Khan N.A.* Cobalt nanoparticles as novel nanotherapeutics against Acanthamoeba castellanii. Parasites Vectors, 2019, **12**: 280-290. https://doi.org/10.1186/s13071-019-3528-2.
9. *Khusnuriyalova A.F., Caporali M., Hey-Hawkins E., Sinyashin O.G., Yakhvarov D.G.* Preparation of Cobalt Nanoparticles.Eur. J. Inorg. Chem.,2021, **30**: 3023–3047. https://doi.org/10.1002/ejic.202100367.
10. *Hatamie S., Dhole S.D., Ding J., Kale S.N.* Encapsulation of cobalt nanoparticles in cross-linked-polymer cages. Journal of Magnetism and Magnetic Materials, 2009, **321**, №14: 2135–2138. doi:10.1016/j.jmmm.2009.01.014.
11. *Carrasco-García A., Vali S.A., Ben-Abbou Z., Moral-Vico J., Markeb A.A., Sánchez A.* Synthesis of Cobalt-Based Nanoparticles as Catalysts for Methanol Synthesis from CO_2 Hydrogenation. Materials, 2024, **17**, №3: 697. https://doi.org/10.3390/ma17030697.
12. *Medvedeva O.I., Kambulova S.S., Bondar O.V., Gataulina A.R., Ulakhovich N.A., Gerasimov A.V., Evtugyn V.G., GilmutdinovI. F., Kutyreva M.P.* Magnetic Cobalt and Cobalt Oxide Nanoparticles in Hyperbranched Polyester Polyol Matrix. Journal of Nanotechnology, 2017, 9 p. doi:10.1155/2017/760765.

13. *Arif M.* Complete life of cobalt nanoparticles loaded into cross-linked organic polymers: a review. RSC Advances 2022, **12,** №24: 15447-15460. https://doi.org/10.1039/D2RA01058E.
14. *Ajmal M., Siddiq M., Al-Lohedan H., Sahiner N.* Highly versatile p(MAc)–M (M: Cu, Co, Ni) microgel composite catalyst for individual and simultaneous catalytic reduction of nitro compounds and dyes. RSC Adv., 2014, **4,** №103: 59562–59570. https://doi.org/10.1039/c4ra11667d.
15. *Farooqi Z.H., Iqbal S., Khan S.R. et al.* Cobalt and nickel nanoparticles fabricated p(NIPAM-co-MAA) microgels for catalytic applications. e-Polymers, 2014, **14**: 313-321. https://doi.org/10.1515/epoly-2014-0111.
16. *Zhao Y.-W., Zheng R.K., Zhang X.X., Xiao J.Q.* A simple method to prepare uniform Co nanoparticles. IEEE Trans. Magn. 2003, **39**: 2764–2766. https://doi.org/10.1109/TMAG.2003.815592.
17. *Kamal T., Khan S.B., Haider S., Alghamdi Y.G., Asiri A.M.* Thin layer chitosan-coated cellulose filter paper as substrate for immobilization of catalytic cobalt nanoparticles. Int. J. Biol. Macromol. 2017, **104**: 56–62. https://doi.org/10.1016/j.ijbiomac.2017.05.157.
18. *Chairam S., Jarujamrus P., Amatatongchai M.* Starch hydrogel-loaded cobalt nanoparticles for hydrogen production from hydrolysis of sodium borohydride. Advances in Natural Sciences: Nanoscienc and Nanotechnology, 2019, **10**, no. 2: 025013. https://doi.org/10.1088/2043-6254/ab23fb.
19. *Lisiecki I., Pileni M. P.* Synthesis of well-defined and low size distribution cobalt nanocrystals: The limited influence of reverse micelles. *Langmuir*, 2003, **19**: 9486–9489. https://doi.org/10.1021/la0301386.
20. *Persson I.* Hydrated metal ions in aqueous solution: How regular are their structures? Pure Appl. Chem., 2010, **82**, №10: 1901–1917. https://doi.org/10.1351/PAC-CON-09-10-22.
21. *Gordon J.E.* Solution Chemistry: The Organic Chemistry of Electrolyte Solutions. Wiley-Interscience, New York, 1975, 554 pp.
22. *Sari N., Kahraman E., Sari B.* Synthesis of Some Polymer-Metal Complexes and Elucidation of their Structures. J. Macromol. Sci., Part A: Pure Appl. Chem., 2006, **43**, no. 8: 1227–1235. https://doi.org/10.1080/10601320600737484.
23. *Lou X., Chen M., Hu B.* The effect of Nitrogen and Oxygen Coordination: Toward a Stable Anode for Reversible Lithium Storage. New J. Chem., 2018, https://doi.org/10.1039/c8nj03367f.
24. *Girma K.B., Lorenz V., Blaurock S., Edelmann F.T.* Coordination Chemistry of Acrylamide: 1. Cobalt(II) Chloride Complexes with Acrylamide - Synthesis and Crystal Structures. Z. Anorg. Allg. Chem., 2005, **631**, no. 8: 1419–1422. https://doi.org/10.1002/zaac.200500027.
25. *Girma K.B., Lorenz V., Blaurock S., Edelmann F.T.* Coordination Chemistry of Acrylamide 4. Crystal Structures and IR Spectroscopic Properties of Acrylamide Complexes with CoII, NiII, and ZnII nitrates. Z. Anorg. Allg. Chem., 2005, **631**, no. 10: 1843–1848. https://doi.org/10.1002/zaac.200500210.
26. *Chen X., Wang L., Li Q., Zhang J., Wang J., Sun J., Zhang Y.* Reversible-deactivation radical polymerizations of acrylamide mediated by cobalt complexes supported by amino-bis(phenolate) ligands. Journal of Macromolecular Science, 2020, Part A, 8 p. https://doi.org/10.1080/10601325.2019.1691453.
27. *Foley K., Condes L., Walters K.B.* Influence of metal-coordinating comonomers on the coordination structure and binding in magnetic poly(ionic liquid)s. Mol. Syst. Des. Eng., 2023, **8**: 1402. https://doi.org/10.1039/d3me00076a.
28. *Zheltonozhskaya T., Permyakova N., Kondratiuk T., Beregova T., Klepko V., Melnik B*. Hybrid-stabilized silver nanoparticles and their biological impact on hospital infections, healing wounds, and wheat cultivation. French-Ukrainian Journal of Chemistry, 2019, **7,** no. 2: 20-39. https://doi.org/10.17721/fujcV7I2P20-39.
29. *Zheltonozhskaya T.B., Permyakova N.M., Kravchenko O.O., Maksin V.I., Nessin S.D., Klepko V.V., Klymchuk D.O.* Polymer/inorganic hybrids containing silver nanoparticles and their activity in the disinfection of fish aquariums/ponds. Polym.-Plast. Technol. Mater, 2020, **59**: 1-23. https://doi.org/10.1080/25740881.2020.1811318.
30. *Zheltonozhskaya T.B., Permyakova N.M., Klepko V.V., Grishchenko L.M., Klymchuk D.O.* Highly dispersed nanocomposites based on polymer/inorganic hybrids and nickel nanoparticles: the role of the matrix structure in the process of formation. Polimernyi Zhurnal, 2023, **45**, no. 1: 37–55. https://doi.org/10.15407/polymerj.45.01.037.
31. *Iler RK.* The chemistry of silica: solubility, polymerization, colloid and surface properties and biochemistry of silica. Wiley-Interscience, 1979, 896 pp.
32. *Xiong B., Loss R. D., Shields D., Pawlik T., Hochreiter R., Zydney A.L., Kumar M.* Polyacrylamide degradation and its implications in environmental systems. *Npj Clean Water,* 2018, **17**: 9 pp. https://doi.org/10.1038/s41545-018-0016-8.
33. *Glavee G.N., Klabunde K.J., Sorensen C.M., Hadjapanayis G.C.* Borohydride reductions of metal ions. A new understanding of the chemistry leading to nanoscale particles of metals, borides, and metal borates. Langmuir, 1992, **8**, no. 3: 771–773. https://doi.org/10.1021/la00039a008.
34. *Gomez-Lahoz C., Garcia-Herruzo F., Rodriguez-Maroto J.M., Rodriguez J.J.* Cobalt(II) removal from water by chemical reduction with sodium borohydride. Water Res., 1993, **27**, №6: 985-992. https://doi.org/10.1016/0043-1354(93)90062-M.

35. *Permyakova N., Zheltonozhskaya T., Revko O., Grischenko L.* Self-assembly and metalation of pH-sensitive double hydrophilic block copolymers with interacting polymer components. Macromol. Symp., 2012, **317–318**, no. 1: 63–74. https://doi.org/10.1002/masy.201100079.
36. *Kelly K.L., Coronado E., Zhao L.L., Schatz G.C.* The Optical Properties of Metal Nanoparticles: The Influence of Size, Shape, and Dielectric Environment.J. Phys. Chem. B, 2003, **107**, no. 3: 668–677. https://doi.org/10.1021/jp026731y.
37. *Liz-Marzan L.M.* Tailoring Surface Plasmons through the Morphology and Assembly of Metal Nanoparticles. Langmuir, 2006, **22**, no. 1: 32–41. https://doi.org/10.1021/la0513353.
38. *Kaminskiene Z, Prosy£evas I., Stonkute J. Guobiene A.* Evaluation of Optical Properties of Ag, Cu, and Co Nanoparticles Synthesized in Organic Medium. Acta Physica Polonica A, 2013, **123**, no. 1: 111–114. https://bibliotekanauki.pl/articles/1400397.pdf.
39. *Zheltonozhskaya T.B., Permyakova N.M., Fomenko A.S., Klymchuk D.O., Klepko V.V., Grishchenko L.N., Vretik L.O.* The process of nickel nanoparticle formation in hydrophilic polymer/inorganic matrices. Molecular Crystals and Liquid Crystals, 2021, **716**, no. 1: 13–28. https://doi.org/10.1080/15421406.2020.1859692.
40. *Wainwright E.* Particle size characterization in turbid colloidal suspensions. Physics Department, The College of Wooster, Ohio, USA, 2014, 7 pp. http://physics.wooster.edu/JrIS/Files/Web_Article_Wainwright.pdf.
41. *Creighton J.A., Eadon D.G.* Ultraviolet-visible absorption spectra of the colloidal metallic elements. J. Chem. Soc. Faraday Trans., 1991, **87**, no. 24: 3881–3891. https://doi.org/10.1039/FT9918703881.

Received 13.12.2023